

steps initially elicit large currents, which then decay rapidly. The rate of deactivation increases with hyperpolarization. In this voltage range, steady-state currents actually decrease with hyperpolarization after passing through a maximum near  $-100$  mV (Fig. 3c). Both observations agree remarkably well with studies on macroscopic skeletal muscle  $\text{Cl}^-$  conductance<sup>1,16</sup>. Currents are predominantly carried by  $\text{Cl}^-$ , as partial replacement of extracellular  $\text{Cl}^-$  by impermeant cyclamate<sup>-</sup> reduces overall current and shifts the reversal potential ( $I=0$ ) towards the new  $\text{Cl}^-$ -equilibrium potential (Fig. 3d). Further, conductance is  $>80\%$  inhibited by  $0.1$  mM 9-anthracene-carboxylic acid (9-AC) (Fig. 3c, d), a  $\text{Cl}^-$ -channel inhibitor. Similar observations were made with macroscopic muscle  $\text{Cl}^-$  conductance, where application of 9-AC elicits myotonia<sup>2,3</sup>.

There are several functional differences between this and the *Torpedo* channel, one being the sensitivity of 9-AC (CIC-0 is inhibited  $<50\%$  by  $2$  mM 9-AC (T.J.J. and G. Schwarz, unpublished results). Although a decrease in open-probability at nega-

tive voltages, as observed with CIC-0, may also explain the current decrease with hyperpolarization for CIC-1, probably the most conspicuous difference is the lack of slow channel activation by hyperpolarization observed with CIC-0 (ref. 4). For CIC-0, this reflects a slow opening of a gate operating on both protochannels of the double-barrelled channel<sup>5,17-19</sup>. Whether this implies that CIC-1 has no double-barrelled structure remains to be elucidated in single-channel studies. This is especially important as most patch-clamp studies on muscle  $\text{Cl}^-$  channels were done on undifferentiated myotubes<sup>20,21</sup> whereas there are no single-channel data on the major  $\text{Cl}^-$  channel from intact differentiated muscle cells.

Thus the muscle  $\text{Cl}^-$  channel CIC-1, although in some regions highly homologous to the *Torpedo* channel CIC-0, has distinct electrophysiological properties. This channel is rather specifically expressed in skeletal muscle and probably provides the major  $\text{Cl}^-$  conductance in that tissue. Its importance for muscle function is best illustrated by the fact that its destruction in mouse mutants leads to myotonia<sup>7</sup>. □

Received 31 July; accepted 27 September 1991.

- Bretag, A. H. *Physiol. Rev.* **67**, 618-724 (1987).
- Rüdel, R. & Lehmann-Horn, F. *Physiol. Rev.* **65**, 310-356 (1985).
- Bryant, S. H. & Morales-Aguilera, A. *J. Physiol., Lond.* **219**, 367-383 (1971).
- Jentsch, T. J., Steinmeyer, K. & Schwarz, G. *Nature* **348**, 510-514 (1990).
- Miller, C. & Richard, E. A. in *Chloride Channels and Carriers in Nerve, Muscle, and Glial Cells* (eds Alvarez-Leefmans, F. J. & Russel, J. M.) 383-405 (Plenum, New York, 1990).
- Conte Camerino, D., De Luca, A., Mambriani, M. & Vrbová, G. *Pflügers Arch.* **413**, 568-570 (1989).
- Steinmeyer, K. *et al. Nature* **354**, 304-308 (1991).
- Kyte, J. & Doolittle, R. F. *J. molec. Biol.* **157**, 105-132 (1982).
- Kimes, B. W. & Brandt, B. L. *Exp. Cell Res.* **98**, 349-366 (1976).
- Cooperman, S. S. *et al. Proc. natn. Acad. Sci. U.S.A.* **84**, 8721-8725 (1987).
- Trimmer, J. S. *et al. Neuron* **3**, 33-49 (1989).
- Trimmer, J. S., Cooperman, S. S., Agnew, W. S. & Mandel, G. *Dev. Biol.* **142**, 360-367 (1990).
- Kallen, R. L. *et al. Neuron* **4**, 233-242 (1990).

- Mishina, M. *et al. Nature* **321**, 406-411 (1986).
- Witzemann, V., Barg, B., Criado, M., Stein, E. & Sakmann, B. *FEBS Lett.* **242**, 419-424 (1989).
- Palade, P. T. & Barchi, R. L. *J. gen. Physiol.* **69**, 325-342 (1977).
- Miller, C. *Phil. Trans. R. Soc. B* **299**, 401-411 (1982).
- Miller, C. & White, M. M. *Proc. natn. Acad. Sci. U.S.A.* **81**, 2772-2775 (1984).
- Bauer, C. K., Steinmeyer, K., Schwarz, J. R. & Jentsch, T. J. *Proc. natn. Acad. Sci. U.S.A.* (in the press).
- Blatz, A. L. & Magleby, K. L. *Biophys. J.* **43**, 237-241 (1983).
- Blatz, A. L. & Magleby, K. L. *Biophys. J.* **47**, 119-123 (1985).
- Kozak, M. *Nucleic Acids Res.* **12**, 857-872 (1984).
- Colman, A. in *Transcription and Translation* (eds Hames, B. D. & Higgins, S. J.) 271-302 (IRL, Oxford, 1984).
- Higuchi, R. in *PCR Technology* (ed. Erlich, H. A.) 61-70 (Stockton, New York, 1989).

ACKNOWLEDGEMENTS. We thank C. Schmekal for technical assistance. This work is supported, in part, by the BMFT, the US Cystic Fibrosis Foundation, the US Muscular Dystrophy Association and the Deutsche Forschungsgemeinschaft.

## Inactivation of muscle chloride channel by transposon insertion in myotonic mice

Klaus Steinmeyer\*, Rainer Klocke†, Christoph Ortland\*, Monika Gronemeier†, Harald Jockusch†, Stefan Gründer\* & Thomas J. Jentsch\*‡

\* Centre for Molecular Neurobiology (ZMNH), Hamburg University, Martinistrasse 52, D-2000 Hamburg 20, Germany

† Developmental Biology Unit, W7, Bielefeld University, PO Box 8640, D-4800 Bielefeld 1, Germany

**MYOTONIA** (stiffness and impaired relaxation of skeletal muscle) is a symptom of several diseases caused by repetitive firing of action potentials in muscle membranes<sup>1</sup>. Purely myotonic human diseases are dominant myotonia congenita (Thomsen) and recessive generalized myotonia (Becker), whereas myotonic dystrophy is a systemic disease. Muscle hyperexcitability was attributed to defects in sodium channels<sup>2,3</sup> and/or to a decrease in chloride conductance (in Becker's myotonia<sup>4</sup> and in genetic animal models<sup>5-10</sup>). Experimental blockage of  $\text{Cl}^-$  conductance (normally 70-85% of resting conductance in muscle<sup>11</sup>) in fact elicits myotonia<sup>1,9</sup>. ADR (ref. 12) mice are a realistic animal model<sup>5-7,12-18</sup> for recessive autosomal myotonia. In addition to  $\text{Cl}^-$  conductance<sup>5</sup>, many other parameters<sup>6,12,16</sup> are changed in muscles of homozygous animals. We have now cloned the major mammalian skeletal muscle chloride channel (CIC-1)<sup>19</sup>. Here we

report that in ADR mice a transposon of the *ETn* family<sup>20-23</sup> has inserted into the corresponding gene, destroying its coding potential for several membrane-spanning domains. Together with the lack of recombination between the *Cic-1* gene and the *adr* locus, this strongly suggests a lack of functional chloride channels as the primary cause of mouse myotonia.

We first investigated whether in myotonic mice changes in the muscle chloride channel gene can be detected by genomic Southern analysis (Fig. 1). Using a rat muscle  $\text{Cl}^-$  channel (CIC-1)<sup>19</sup> probe, aberrant fragments were indeed found in ADR (*adr/adr*) mice with several restriction nucleases, and with one enzyme in myotonic mice carrying the allelic mutation *adr*<sup>mt0</sup> (ref. 24). No rearrangement was found with the *adr*<sup>K</sup> (ref. 25) allele. With ADR, aberrant fragments were always larger than the wild-type fragment, suggesting an insertional mutation. A total of 55 ADR mice were tested. In each of these the 6.6-kilobase (kb) *EcoRI* fragment was replaced by the 10.5-kb fragment, which was never found in any homozygous wild-type laboratory mouse. In proven heterozygous A2G mice, both the 6.6- and the 10.5-kb fragments were present.

Northern analysis was used to examine  $\text{Cl}^-$  channel messenger RNAs in various myotonic mouse strains. A probe from the 5' end of CIC-1 detected a roughly 4.5-kb message in skeletal muscle of both normal mice and myotonic mice homozygous for *adr*<sup>mt0</sup> and *adr*<sup>K</sup>, whereas several bands were apparent with *adr/adr* mice (a roughly 7-8-kb doublet, and another doublet at about 1.6-2.0 kb) (Fig. 2a, d). Heterozygous (phenotypically normal) mice (*adr/+*) additionally had normal transcripts (about 4.5 kb), which were missing in homozygous (*adr/adr*) muscle. The sizes of the small mRNAs (1.6-2.0 kb) are insufficient to encode a functional  $\text{Cl}^-$  channel<sup>19,26</sup>. To examine the *adr* mutation in detail, a complementary DNA library from (*adr/adr*) skeletal muscle was screened with CIC-1 cDNAs<sup>19</sup>. All 11 clones isolated were homologous to the rat muscle  $\text{Cl}^-$  channel cDNA 5' to the sequence encoding the ninth putative

‡ To whom correspondence should be addressed.

transmembrane domain (D9), but no homologous sequence 3' to D9 was found. Four cDNAs extended into D9 (Fig. 3), but diverged (to two different sequences) after the triplet encoding lysine (amino-acid 467 in the rat<sup>19</sup>). This position corresponds exactly to an exon-intron boundary in the rat channel, suggesting that in ADR mice this exon is spliced to sequences unrelated to the Cl<sup>-</sup> channel. Database searches showed that these are nearly identical with known members of the *ETn* family of mouse transposons<sup>20-23</sup>. High homology exists to an *ETn* sequence which had inserted into the switch region of immunoglobulins<sup>23</sup>. In other regions, where no sequence information for this particular transposon is available, we found near identity to a fully sequenced genomic clone (MG1) of another *ETn* transposon<sup>22</sup>. We assume that a single transposon, which displays high homology to the first member and continues as MG1, has inserted into the Cl<sup>-</sup>-channel gene.

Among the four cDNAs examined, three different splice variants were found (Fig. 3). Two clones (*cDNA* 2 and 3), using the polyadenylation site in one of the long terminal repeats (LTR) of *ETn*, terminated with poly(A) tails. The predicted mRNA lengths are about 1.6 kb and 1.8 kb, corresponding to the small doublet in northern blots (Fig. 2). The *cDNA* 1 originated from splicing into *ETn* shortly downstream of the 5' LTR polyadenylation site, and the mRNA may continue until the 3' LTR polyadenylation signal. This could explain the long (roughly 7 kb) transcripts detected in northern blots. Thus insertion of a transposon (probably into the intron in D9) leads to abnormal splice products in which the sequence 3' of D9 is

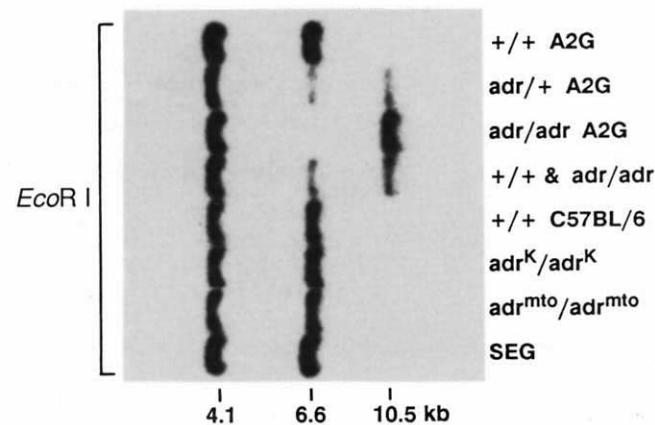


FIG. 1 Southern blot analysis of chloride channel gene *CIC-1* in different mouse strains and mutants. DNAs were from normal and myotonic mice for which the genotypes and genetic backgrounds are indicated (SEG = *Mus spretus*). *EcoRI* digestion reveals aberrant restriction fragments in ADR mice and *adr/+* heterozygotes. In the lane designated '+/+ & *adr/adr*', a 1:1 mixture of A2G +/+ and A2G *adr/adr* DNAs was analysed. Aberrant restriction fragments were detected in ADR mice with the following nucleases (fragment-length, mutant (kb)/fragment length, normal (kb)): *Bam*HI (13/11.5), *Eco*RI (10.5/6.6), *Pst*I (7.4/5.8) and *Ssp*I (4.5/3.5). No differences were found with *Bcl*II, *Bgl*III, *Eco*RV, *Hinc*II, *Hind*III, *Hpa*I, *Msp*I, *Pvu*II, *Rsa*I, *Scal*I, *Sst*I, *Stu*I, *Taq*I or *Xba*I. In myotonic mice homozygous for the *adr*<sup>mt0</sup> or *adr*<sup>K</sup> mutations, no abnormal fragments were found with any of these nucleases, but *Hinc*II detected an abnormal fragment in *adr*<sup>mt0</sup>. Lengths of fragments are indicated.

**METHODS.** A2G mice carrying the recessive autosomal mutation, 'arrested development of righting response' (*adr*)<sup>12</sup>, were obtained from R. L. Watts and D. L. Watts, Guy's Hospital, London. SWR/J mice carrying the allele *adr*<sup>mt0</sup> (ref. 24) were from the Jackson Laboratory, Bar Harbor, ME. The *adr*<sup>mt0</sup> gene was outbred into the more vigorous inbred strain C57BL/6J. The *adr*<sup>K</sup> breeders<sup>25</sup> (noninbred background) were obtained from P. Neumann, Harvard Medical School. DNAs were prepared from lungs. About 10 µg digested DNA was separated on a 0.8% agarose gel, blotted onto a nylon membrane and hybridized with a <sup>32</sup>P-labelled *CIC-1* (ref. 19) probe extending from 970 to 1,881 bp of the rat sequence.

replaced by *ETn* sequences. To ascertain that the Cl<sup>-</sup>-channel sequence 3' to D9 is missing in all ADR transcripts, we probed the northern blot with a 3' cDNA. No signal was found with homozygous ADR animals, whereas the normal ~4.5-kb message was detected in normal mice, heterozygous *adr/+* animals and homozygous animals of other myotonic strains (Fig. 2b). An *ETn* probe detected transcripts only in *adr/adr* and *adr/+* RNA (Fig. 2c, e). They corresponded exactly to those recognized by the 5' Cl<sup>-</sup>-channel probe. Thus, all detectable Cl<sup>-</sup>-channel mRNA is functionally destroyed in ADR mice.

Using interspecies backcrosses, we mapped the *Clc-1* locus on mouse chromosome 6 between marker genes *Tcrb* and *Hox-1.1*, 1.3 centiMorgans (cM) ± 1.0 cM from *Tcrb* (Fig. 4). This is

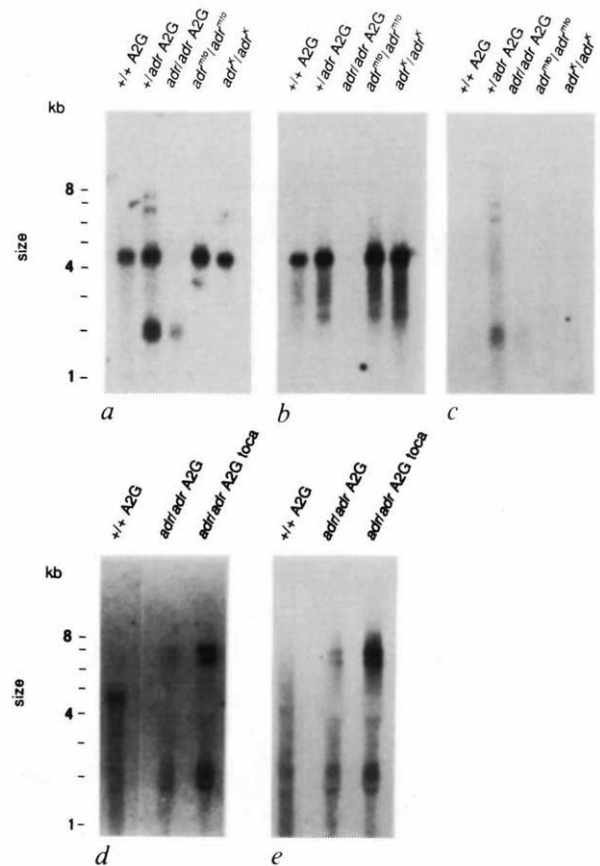


FIG. 2 Northern analysis of muscle Cl<sup>-</sup>-channel RNAs in normal and myotonic mice. Skeletal muscle RNA from the mouse strains indicated were analysed by probing blots with a rat skeletal muscle chloride channel (*CIC-1*) probe 5' to D9 (a, d), a *CIC-1* probe 3' to D9 (b) and a probe derived from *ETn* sequences (c, e). a-c derive from the same blot hybridized sequentially with different probes. The mRNAs analysed on the blot used for d and e is from individuals different from those of a-c.

**METHODS.** RNA was isolated from leg skeletal muscle of adult mice of the indicated strains. (*adr/adr*) toxa indicates homozygous ADR mice treated for 29 days with 1.5 mg tocanide per g dry food, which partially reverts the myotonic phenotype<sup>13,16</sup>. About 3 µg poly (A)<sup>+</sup> RNA (a-c) or 30 µg total RNA (d, e) per lane were electrophoresed on denaturing agarose gels, blotted onto nylon membranes and probed with <sup>32</sup>P-labelled cDNA probes. The 5' probe extends from -83 to 1,137 bp, and the 3' probe from 1,542 to 3,523 bp of the rat *CIC-1* sequence<sup>19</sup>. The *ETn* probe is derived from clone *cDNA*2, extending from the *Xba*I site immediately after the first splice site (equivalent to position 268 of *ETn* A) to the poly(A) tail. Equal loading and absence of degradation was checked by ethidium bromide staining, but control hybridization with a  $\gamma$ -actin cDNA gave weaker signals for lanes 1 and 3 (a-c) and lanes 2 (d, e); the amounts of transcripts in these lanes may thus be underestimated by a factor of about 3.



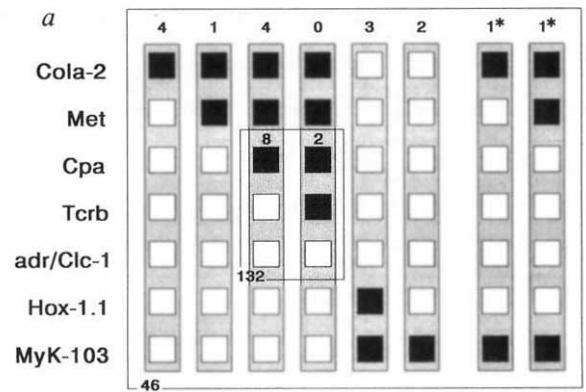
other parameters<sup>6,12,16</sup> were altered. Some changes were shown to be secondary to muscle hyperactivity<sup>16</sup>. In addition to a mutated Cl<sup>-</sup> channel, several other mechanisms have been considered to cause myotonia<sup>6,15</sup>. This work demonstrates the pleiotropic effects a defect in a single ion channel can have.

Thus *ETn* insertion has been shown to cause inheritable disease. *ETn* transposons were first identified as transcripts in teratocarcinoma cells<sup>20</sup> and during early embryonic development<sup>21</sup>. In these cases, a single polyadenylated RNA of  $\geq 5$  kb is transcribed, starting from a promoter in *ETn*. Here, of course, the Cl<sup>-</sup>-channel promoter is used. Interestingly, differential splicing also occurs in *ETn*, suggesting an important influence of *cis* sequences on the use of potential splice sites. Although Cl<sup>-</sup>-channel inactivation by *ETn* insertion is unique for the *adr* mutation, it is clear that in *adr*<sup>mto</sup> and *adr*<sup>K</sup>, whose mutation is allelic to *adr*, the defect also resides in the Cl<sup>-</sup> channel and will be due to other types of mutations (such as point mutations).

ADR mice are a realistic animal model<sup>6,7</sup> for human recessive generalised myotonia, which displays the same mode of inheritance and a reduced muscle Cl<sup>-</sup> conductance<sup>4</sup>, though changes in Na<sup>+</sup> channels were also described<sup>3</sup>. Both changes in Cl<sup>-</sup> conductance<sup>28</sup> and Na<sup>+</sup> channels<sup>2</sup> were also observed with myotonia congenita, a dominant disease. If these diseases were due to Cl<sup>-</sup>-channel defects, they would be expected to map to

◀ FIG. 3 Mechanism of Cl<sup>-</sup>-channel inactivation in ADR mice. *a*, Sequence analysis of splice variants. Sequences of three ADR cDNAs (cDNA 1–3) are compared with the rat muscle Cl<sup>-</sup>-channel sequence (rat mus)<sup>19</sup> to a rat genomic clone, and to two members of the *ETn* family of transposable elements (*ETn* Ig, transposon encountered in the switch region of an immunoglobulin gene<sup>23</sup>, GeneBank accession number M29266; *ETn* A, sequence of genomic clone MG1 (ref. 22), GeneBank accession No. M16478). Where appropriate, the corresponding protein translation is shown (the rat channel is compared at the protein level only). Putative transmembrane spans are indicated (D7 to D9). Only differences in sequence are shown; dashes indicate gaps, and points identities. The polyadenylation site in the LTR is underlined; splice consensus sequences are highlighted by lower case letters; IR, the inverted repeat; numbers, equivalent base pairs in *ETn* A. Predicted *adr* translation products are >95% identical to the rat muscle Cl<sup>-</sup>-channel protein until it reaches the exon–intron boundary in D9. In cDNA 1 and 2 the exon is spliced into the 5' LTR of an *ETn* transposon at the same position (268). cDNA 2 leaves 167 bases downstream by splicing into the 3' LTR (where *ETn* Ig and *ETn* A are nearly identical). It continues until it is polyadenylated. cDNA 1 continues to be highly homologous to *ETn* Ig over the entire range where sequence information for this transposon is available. More downstream, sequence identity to *ETn* A is found. cDNA 3 splices directly into the (3' or 5') LTR and is polyadenylated. cDNA 2 and 3 splice into different reading frames of *ETn*, resulting in different translations. In all three splice variants, stop codons are encountered. *b*, Model for Cl<sup>-</sup>-channel inactivation in ADR mice. Top, proposed genomic structure with *ETn* transposon (of about 5.5 kb total length) having inserted somewhere into the Cl<sup>-</sup>-channel intron disrupting the sequence encoding putative transmembrane domain D9. IR, inverted repeats; LTR, long terminal repeat; AATAAA, polyadenylation site. Below, schematic representation of splice variants cDNA 1–3. As sequences in both LTRs are nearly identical, two splice mechanisms cannot be distinguished for cDNA 3 (one is depicted by a dashed line).

**METHODS.** A cDNA library in  $\lambda$ gt10 was constructed (clontech) by oligo (dT) and random primed synthesis starting from 7  $\mu$ g poly (A)<sup>+</sup> RNA from ADR skeletal muscle. About 2  $\times 10^6$  primary recombinants were screened with a mixture of radiolabelled rat muscle Cl<sup>-</sup>-channel cDNAs<sup>19</sup> covering most of the coding sequence (extending from bp 432 to 632, and from bp 982 to 2287). About 60 positive clones were identified, 11 of which were isolated and sequenced from both ends. Four clones (named cDNA 1–4) extending into domain D9 were sequenced using T7 DNA polymerase. cDNA 3 and 4 represented identical splice variants. Only relevant regions were sequenced. The clones began at the following 5' positions (numbers according to the rat channel<sup>19</sup>): cDNA 1, 383 bp; cDNA 2, –37 bp; and cDNA 3, –65 bp. For genomic analysis, a rat genomic library in EMBL3 was screened using a rat Cl<sup>-</sup>-channel cDNA<sup>19</sup>. The sequence shown was obtained from a *Hind*III fragment which was subcloned into pBluescript. The sequences have been deposited in the EMBL/GenBank database under accession numbers: X62895, X62896 and X62897.



*b* mouse Chr 6 human Chr 7

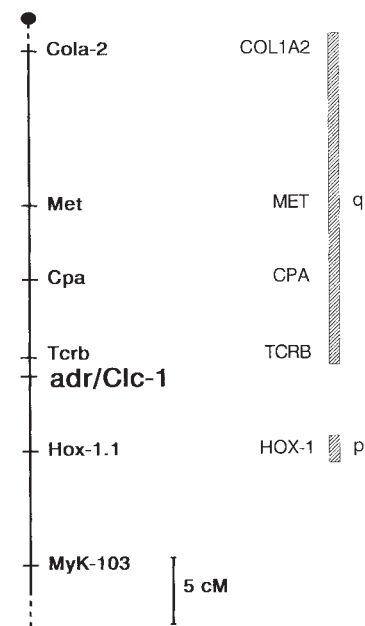


FIG. 4 Mapping of the *adr/Clc-1* gene on mouse chromosome 6 using interspecies backcross (BC). *a*, Schematic representation of experimental results used to map the locus. Recombinant haplotypes (indicated by vertical bars) of *Mus musculus domesticus* (Mmd)  $\times$  *Mus spretus* (SEG/1) BC individuals are shown. Marker genes tested are given at left. Observed numbers of recombinants are indicated at the top of each haplotype. Empty squares indicate that the marker gene allele originated from the same species as the *adr/Clc-1* allele (no recombination), filled squares indicate a different origin (recombination). Asterisks indicate double recombinants. Frames indicate sets of marker genes tested, with inserted numbers indicating total numbers of backcross individuals on which these tests were performed, that is all markers shown at left were tested on 46 individuals, whereas 3 markers (*Cpa*, *Tcrb*, *adr/Clc-1*) were tested on 132 individuals, including the 46 ADR animals in the outer frame. Outer frame shows a result of a (Mmd A2G *adr*/+  $\times$  SEG/1 +/+)  $\times$  Mmd A2G *adr*/+ BC, in which the ADR phenotype was used to indicate the *Mus musculus domesticus* origin of the F<sub>1</sub>-derived allele of *adr*. Inner frame represents results from the combined scores of ADR phenotypes and *Clc-1* alleles (which now became possible), and are in part (72 individuals) derived from a (C57BL/6J  $\times$  SEG/1)  $\times$  C57BL/6J BC (see ref. 29). *b*, Genetic map of proximal mouse chromosome 6, as based on recombination data from 150 BC individuals part of which are shown in *a*, compared with regions of human chromosome 7 to show conserved synteny (from ref. 18).

**METHODS.** DNAs from BC individuals were isolated and analysed by Southern blotting as described in Fig. 1. Mapping was done previously on a limited number of individuals using the myotonic phenotype to identify the *adr* locus<sup>18</sup>; it could now be extended exploiting species differences in *Xba*I fragments detected by the *Clc-1* probe. Marker gene probes: *Cola-2*, probe NJ3 3.2, human<sup>30</sup>; *Met*, pmtd, human<sup>31</sup>; *Cpa*, murine<sup>32</sup>; *Tcrb*, human<sup>33</sup>; *Hox-1.1*, pHox1-B2.8 murine<sup>34</sup>; *Myk-103*, Bgl 1.6 murine<sup>35</sup>.

human chromosome 7 (Fig. 4). It is now possible to address these issues directly. □

Received 31 July; accepted 27 September 1991.

- Rüdel, R. & Lehmann-Horn, F. *Physiol. Rev.* **65**, 310–356 (1985).
- Iaizzo, P. A. *et al. Neuromusc. Disord.* **1**, 47–53 (1991).
- Franko, C. *et al. Muscle Nerve* **14**, 762–770 (1991).
- Rüdel, R., Ricker, K. & Lehmann-Horn, F. *Muscle Nerve* **11**, 202–211 (1988).
- Mehrke, G., Brinkmeier, H., & Jockusch, H. *Muscle Nerve* **11**, 440–446 (1988).
- Jockusch, H. in *The Dynamic State of Muscle Fibers* (ed. Pette, D.) 429–443 (Walter de Gruyter, New York, 1990).
- Rüdel, R. *Trends Neurosci.* **13**, 1–3 (1990).
- Lipicky, R. J. & Bryant, S. H. *J. gen. Physiol.* **50**, 89–111 (1966).
- Bryant, S. H. & Morales-Aguilera, A. *J. Physiol., Lond.* **219**, 367–383 (1971).
- Adrian, R. H. & Bryant, S. H. *J. Physiol., Lond.* **240**, 505–515 (1974).
- Bretag, A. H. *Physiol. Rev.* **67**, 618–724 (1987).
- Watkins, W. J. & Watt, D. C. *Lab. Anim.* **18**, 1–6 (1984).
- Reininghaus, J., Fuchtbauer, E.-M., Bertram, K. & Jockusch, H. *Muscle Nerve* **11**, 433–439 (1988).
- Fuchtbauer, E.-M., Reininghaus, J. & Jockusch, H. *Proc. natn. Acad. Sci. U.S.A.* **85**, 3880–3884 (1988).
- Brinkmeier, H. & Jockusch, H. *Biochem. biophys. Res. Commun.* **148**, 1383–1389 (1987).
- Jockusch, H., Reininghaus, J., Stuhlfauth, I. & Zippel, M. *Eur. J. Biochem.* **171**, 101–105 (1988).

- Költgen, D., Brinkmeier, H. & Jockusch, H. *Muscle Nerve* **14**, 775–780 (1991).
- Jockusch, H., Schenk, S. & Gronemeier, M. *Mouse Genome* **66**, 216 (1990).
- Steinmeyer, K., Ortlund, C. & Jentsch, T. *J. Nature* **354**, 301–304 (1991).
- Brület, P., Kaghad, M., Xu, Y.-S., Croissant, O. & Jacob, F. *Proc. natn. Acad. Sci. U.S.A.* **80**, 5641–5645 (1983).
- Brület, P., Condamine, H. & Jacob, F. *Proc. natn. Acad. Sci. U.S.A.* **82**, 2054–2058 (1985).
- Sonigo, P. *et al. Proc. natn. Acad. Sci. U.S.A.* **84**, 3768–3771 (1987).
- Shell, B., Szurek, P. & Dunnick, W. *Molec. cell. Biol.* **7**, 1364–1370 (1987).
- Heller, A. H., Eicher, E. M., Hallett, M. & Sidman, R. L. *J. Neurosci.* **2**, 924–933 (1982).
- Neumann, P. & Weber, T. *Mouse News Lett.* **83**, 157 (1989).
- Jentsch, T. J., Steinmeyer, K. & Schwarz, G. *Nature* **348**, 510–514 (1990).
- Conte Camerino, D., De Luca, A., Mambriani, M. & Vrbová, G. *Pflügers Arch.* **413**, 568–570 (1989).
- Lipicky, R. J., Bryant, S. H. & Salmon, J. H. *J. clin. Invest.* **50**, 2091–2103 (1971).
- Friedmann, J. M., Leibel, R. L. & Bahary, N. *Mammalian Genome* **1**, 130–144 (1991).
- Meyers, J. C. *et al. Proc. natn. Acad. Sci. U.S.A.* **78**, 3516–3520 (1981).
- Dean, M. *et al. Nature* **318**, 385–388 (1985).
- Quinto, C. *et al. Proc. natn. Acad. Sci. U.S.A.* **79**, 31–35 (1982).
- Yanagi, Y. *et al. Nature* **308**, 145–149 (1984).
- Bucan, M. *et al. EMBO J.* **5**, 2899–2905 (1986).
- Wilkie, T. M. & Palmiter, R. D. *Molec. cell. Biol.* **7**, 1646–1655 (1987).

ACKNOWLEDGEMENTS. We thank C. Schmekal for technical assistance, K. Kaupmann and S. Schenk for interspecies hybrids and M. Koch, F. Ramirez, J. H. Friedmann, A. Püschel, R. B. Palmiter and L. C. Tsui for marker gene probes. Work in T.J.J.'s laboratory is supported by the BMFT, the US Cystic Fibrosis Foundation, the US Muscular Dystrophy Association and the DFG, and in H.J.'s laboratory by the DFG.

## Peripheral deletion of self-reactive B cells

David M. Russell\*, Zlatko Demčić†, Grant Morahan‡, J. F. A. P. Miller‡, Kurt Bürki§ & David Nemazee\*||¶

\* Division of Basic Sciences, Department of Pediatrics, National Jewish Center for Immunology and Respiratory Medicine, 1400 Jackson Street, Denver, Colorado 80206, USA

† Department of Molecular Biology, Hoffmann-La Roche, CH-4005 Basel, Switzerland

‡ Walter and Eliza Hall Institute of Medical Research, The Royal Melbourne Hospital, Victoria 3050, Australia

§ Department of Biotechnology, Sandoz, CH-4002 Basel, Switzerland

|| Department of Microbiology and Immunology, University of Colorado Health Sciences Center, Denver, Colorado 80206, USA

¶ To whom correspondence should be addressed

**B LYMPHOCYTES are key participants in the immune response because of their specificity, their ability to take up and present antigens to T cells, and their capacity to differentiate into antibody-secreting cells. To limit reactivity to self antigens, auto-specific B cells can be functionally inactivated or deleted<sup>1–4</sup>. Developing B cells that react with membrane antigens expressed in the bone**

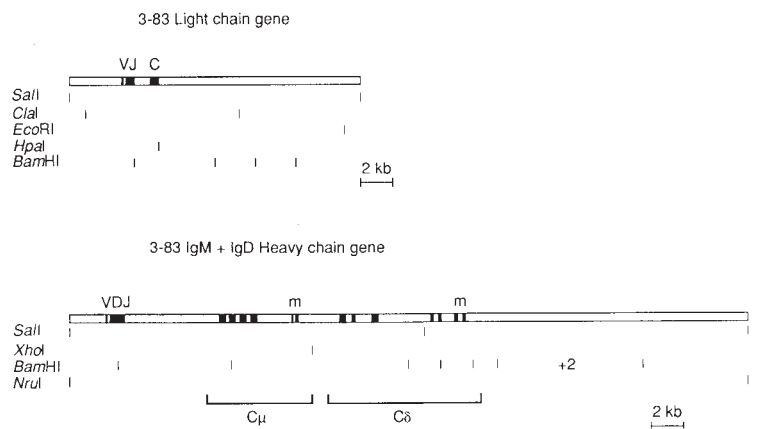
marrow are deleted from the peripheral lymphocyte pool<sup>4–6</sup>. It is important to ascertain the fate of B cells that recognize membrane autoantigens expressed exclusively on peripheral tissues because B cells in the peripheral lymphoid organs are phenotypically and functionally distinct from bone-marrow B cells<sup>7–9</sup>. Here we show that in immunoglobulin-transgenic mice, B cells specific for major histocompatibility complex class I antigen can be deleted if they encounter membrane-bound antigen at a post-bone-marrow stage of development. This deletion may be necessary to prevent organ-specific autoimmunity.

To test for peripheral deletion double-transgenic (Dbl-Tg) mice were produced by mating mice bearing the *MT-K<sup>b</sup>* transgene, which targets expression of the membrane major histocompatibility complex (MHC) class I antigen *K<sup>b</sup>* to the liver<sup>10</sup>, with 3-83 $\mu\delta$  mice (Ig-Tg), which are transgenic for heavy and light chain immunoglobulin genes encoding anti-*K<sup>b</sup>* antibody (see legend to Fig. 1). No messenger RNA or surface-protein expression of the *K<sup>b</sup>* is detectable in lymphoid tissues of *MT-K<sup>b</sup>* mice<sup>10</sup>. Both the Ig-Tg and *MT-K<sup>b</sup>* transgenics were bred as hemizygous traits and (Ig-Tg  $\times$  *MT-K<sup>b</sup>*)F<sub>1</sub> littermates were analysed.

Double-transgenic Ig-Tg/*MT-K<sup>b</sup>* mice deleted peripheral B cells. In Dbl-Tg lymph nodes there were >25-fold fewer cells bearing IgM (sIgM<sup>+</sup> cells) compared with Ig-Tg or non-Tg controls and there were no detectable 3-83 idiotype-positive cells

FIG. 1 Maps of the DNA fragments used to generate 3-83 $\mu\delta$  transgenic mice. Dark regions represent exons.

**METHODS.** Mice were produced using functional rearranged heavy- and light-chain genes encoding the 3-83 antibody. This antibody binds with moderate affinity to *K<sup>k</sup>*, with weak affinity to *K<sup>b</sup>*, and fails to bind to H-2<sup>d</sup> cells<sup>22</sup>. Transgenic mice encoding the IgM form of 3-83 have been described<sup>4–6</sup>. Self tolerance to *K<sup>k</sup>* and *K<sup>b</sup>* in the IgM-only 3-83 mice is mediated by deletion in H-2<sup>d</sup> transgenic  $\rightarrow$  H-2<sup>d</sup>  $\times$  H-2<sup>k</sup> or H-2<sup>d</sup> transgenic  $\rightarrow$  H-2<sup>d</sup>  $\times$  H-2<sup>d</sup> bone marrow chimaeras<sup>5,6</sup>. To generate the 3-83 IgM plus IgD heavy-chain fragment, the 3-83 $\mu$  construct used previously<sup>4</sup> was extended to include the complete *C $\delta$*  genomic locus. The 3-83 $\mu$  insert was liberated from its vector by partial digestion with *EcoRI* and cloned into the *EcoRI* site of  $\lambda$ EMBL3 to generate  $\lambda$ 241. A cosmid clone spanning the (DBA/2-derived) Ig-*C $\mu$*  and Ig-*C $\delta$*  regions was then isolated from a genomic library of the T-cell hybrid BDF1 16 (ref. 23), linearized with *XhoI*, which cuts at the site between *C $\mu$*  and *C $\delta$* , and ligated together with the *VDJ/C $\mu$* -containing *SalI/XhoI* fragment of  $\lambda$  241 and with *SalI*-digested pNKL cosmid vector<sup>24</sup>, resulting in a cosmid whose restriction map in the *C $\mu$ /C $\delta$*  region corresponds to the natural locus. The 42-kilobase (kb) insert was liberated from all but ~200 base pairs (bp) of the vector by *NruI* digestion. Light- and heavy-chain



gene fragments were isolated and transgenic mice produced as described<sup>4</sup>. Southern blotting and segregation analysis indicated that the 3-83 $\mu\delta$  line has ~3–5 copies of the light- and heavy-chain genes co-integrated at a single chromosomal locus. m, Transmembrane exons.